Research in Emerging and Applied Technologies
https://reatjournal.com

Drone Inspection Workflows and Maintenance Efficiency in Solar Farm Operations

Noah Rogers*

Faculty of Engineering and Physical Sciences, University of Leeds, Leeds, England, United Kingdom

Corresponding author: noah.rogers@leeds.ac.uk

Abstract

The rapid expansion of utility-scale solar farms necessitates advanced, highly efficient maintenance strategies to ensure optimal energy yield and system longevity. While unmanned aerial vehicles equipped with thermographic sensors have revolutionized defect detection by rapidly identifying thermal anomalies across vast photovoltaic arrays, a critical gap remains in translating these surface-level thermal observations into predictive structural health assessments. This paper investigates the integration of drone inspection workflows with finite element modeling to dynamically assess the mechanical degradation of solar modules induced by thermal stress. By acquiring high-resolution thermographic data from an operational solar farm, this study maps localized temperature gradients onto a multi-layered finite element model of photovoltaic panels. The structural simulation analyzes the thermal-mechanical stress propagation through the glass cover, encapsulant layers, silicon cells, and backsheet. Findings indicate that coupling aerial thermography with finite element analysis allows operators to distinguish between benign thermal fluctuations and structurally critical hotspots that threaten module integrity. This synergistic approach significantly enhances maintenance efficiency by enabling targeted, predictive interventions rather than relying on scheduled or reactive maintenance. The proposed methodology optimizes resource allocation, minimizes operational downtime, and extends the overall lifecycle of photovoltaic infrastructure, providing a robust framework for next-generation solar farm management.

Keywords: Unmanned Aerial Vehicles; Photovoltaic Systems; Finite Element Method; Predictive Maintenance; Drone Inspection Workflows

1. Introduction

1.1 Background on Solar Farm Maintenance

The global transition toward sustainable energy sources has precipitated an unprecedented proliferation of utility-scale photovoltaic installations. As these solar farms grow in both spatial footprint and energy capacity, they encounter increasingly complex operational and maintenance challenges. The continuous exposure of photovoltaic modules to harsh environmental conditions, including extreme temperature fluctuations, mechanical wind loads, hail impact, and ultraviolet radiation, invariably leads to material degradation over time. Common anomalies such as microcracks, delamination, snail trails, and defective bypass diodes not only compromise the structural integrity of individual panels but also cause severe power degradation across interconnected strings. Traditional maintenance paradigms have predominantly relied on manual visual inspections or handheld thermography, methodologies that are prohibitively time-consuming, labor-intensive, and susceptible to human error. In expansive solar facilities spanning hundreds of acres, relying on ground-based inspection crews results in prolonged inspection cycles, delayed defect identification, and significant revenue losses due to suboptimal power generation. Consequently, the industry is urgently pivoting toward automated, scalable diagnostic technologies capable of rapid data acquisition and accurate anomaly classification. The imperative to maximize the return on investment for renewable energy infrastructure necessitates a paradigm shift from reactive and time-based maintenance scheduling to highly optimized, condition-based predictive maintenance frameworks [1].

1.2 Role of Unmanned Aerial Vehicles

The integration of unmanned aerial vehicles into the operational workflows of the renewable energy sector represents a transformative advancement in asset monitoring. Equipped with high-resolution radiometric thermal cameras and high-definition visual sensors, industrial-grade drones can systematically traverse large-scale solar arrays, capturing comprehensive diagnostic data in a fraction of the time required by terrestrial inspection teams [2]. These aerial platforms follow pre-programmed autonomous flight paths, ensuring consistent spatial coverage, optimal sensor overlap, and precise georeferencing of acquired imagery. Through the application of photogrammetry and radiometric image processing, operators can generate detailed orthomosaics and thermal maps that highlight temperature anomalies across the entire solar facility. Since electrical faults, cellular damage, and shading effects typically manifest as localized heat concentrations or hotspots on the surface of the photovoltaic module, aerial thermography provides a rapid, non-destructive mechanism for pinpointing defective components [3]. However, while the deployment of unmanned aerial vehicles resolves the logistical bottleneck of data collection, the resultant thermal imagery remains inherently diagnostic rather than prognostic. It identifies where abnormal heating occurs but falls short of predicting the imminent structural consequences of these temperature gradients on the layered architecture of the solar panel [4].

1.3 Problem Statement and Objectives

Despite the widespread adoption of drone-based thermography, a critical analytical void persists between the identification of a thermal anomaly and the formulation of an optimized maintenance response. Maintenance managers frequently struggle to categorize the severity of detected hotspots, leading to either premature panel replacement, which squanders operational budgets, or delayed intervention, which risks catastrophic module failure and cascading electrical issues. The fundamental problem lies in the inability to quantify the internal mechanical stress generated by external temperature differentials. To bridge this gap, this study proposes a novel conceptual and methodological framework that links drone inspection workflows directly to finite element modeling [5]. Finite element modeling is an advanced computational technique that can simulate the physical behavior of complex structures under specific environmental loads. By utilizing real-world thermal data harvested from drone inspections as boundary conditions within a finite element simulation of a photovoltaic module, this research aims to accurately model the thermal-mechanical stress distribution across the panel materials. The primary objective is to demonstrate that integrating finite element analysis into the drone inspection pipeline enables a highly granular understanding of defect severity. This deep structural insight is expected to revolutionize maintenance efficiency by providing actionable intelligence, optimizing workforce deployment, minimizing unnecessary replacements, and safeguarding the long-term energy yield of solar farm operations.

2. Literature Review and Theoretical Framework

2.1 Evolution of Photovoltaic Inspection Techniques

The historical trajectory of photovoltaic inspection methodologies reflects a continuous quest for greater accuracy, speed, and cost-effectiveness. In the nascent stages of the solar industry, maintenance operations were heavily reliant on manual visual checks. Technicians would physically walk the rows of solar arrays, scrutinizing panels for visible signs of damage such as shattered glass, discoloration, or heavy soiling. This approach, while straightforward, was grossly inadequate for detecting internal electrical faults or microcracks that leave no visible footprint on the module surface [6]. As the industry matured, current-voltage curve tracing and electroluminescence imaging were introduced. Current-voltage tracing measures the electrical output of a string to identify performance deviations, whereas electroluminescence involves applying a reverse current to the panel in a dark environment to capture infrared emissions, revealing deep structural defects [7]. While highly accurate, electroluminescence imaging is extremely disruptive, requiring operations to be halted and panels to be individually tested, making it unfeasible for routine, large-scale deployment.

The advent of thermography marked a significant turning point. Initially conducted using handheld thermal cameras, this technique leveraged the principle that electrical inefficiencies and physical defects in solar cells generate localized resistance, which dissipates as heat. Handheld thermography allowed for non-contact, operational inspection [8]. However, as solar farms scaled up to utility levels, the slow pace of terrestrial thermography became a limiting factor. The subsequent transition to drone-based platforms equipped with radiometric sensors consolidated the benefits of thermography with the speed and scalability of aviation. Drones enabled the inspection of megawatts of installed capacity in a single day. Yet, as the volume of inspection data exploded, the analytical bottleneck shifted from data collection to data interpretation. Current literature extensively documents the application of machine learning algorithms for the automated detection and classification of thermal anomalies in drone imagery, but these studies predominantly focus on computer vision techniques rather than the underlying physics of material degradation [9].

2.2 Drone Workflows in Renewable Energy

The standard operating procedure for drone inspections in renewable energy environments involves several meticulously planned phases. Initially, mission planning software is utilized to define the geographical boundaries of the inspection zone, determine the optimal flight altitude, and establish the required forward and side image overlap to ensure accurate photogrammetric reconstruction [10]. Environmental parameters, particularly solar irradiance and wind speed, must be strictly monitored, as sufficient and steady sunlight is required to generate the necessary thermal contrast for anomaly detection. Following the flight execution, the raw radiometric data undergoes a complex processing pipeline. The images are geometrically corrected, stitched into comprehensive thermal maps, and cross-referenced with visual imagery to filter out false positives caused by transient shading, bird droppings, or heavy localized soiling.

Recent scholarly contributions have emphasized the integration of geographical information systems into this workflow, enabling the precise localization of defective modules within the vast array topology. This spatial awareness is crucial for generating actionable maintenance tickets. However, the existing literature highlights a significant limitation in the current operational paradigm. The workflow typically terminates at the anomaly classification stage, yielding a simple inventory of hotspots categorized by temperature delta thresholds. Authors have pointed out that relying solely on temperature differentials is an oversimplification [11]. A high-temperature hotspot does not unequivocally equate to immediate structural failure, just as a lower-temperature anomaly might induce critical stress if located near a mechanical mounting point or existing microcrack. The lack of a mechanistic understanding of how these thermal gradients interact with the multi-material composition of the solar panel represents a fundamental barrier to achieving true predictive maintenance [12].

2.3 Finite Element Modeling in Predictive Maintenance

Finite element modeling has long been established as a cornerstone of structural engineering, aerospace design, and mechanical failure analysis. It involves mathematically discretizing a continuous structural domain into a finite number of smaller, simpler components called elements, which are interconnected at specific points known as nodes. By solving the governing equations of physics across this network, finite element modeling can predict how a complex structure will respond to various external stimuli, including mechanical loads, vibrations, and thermal fluctuations [13]. In the context of photovoltaic research, finite element modeling has traditionally been utilized during the manufacturing and design phases to optimize the thickness of the glass cover, select appropriate encapsulant materials, or evaluate the panel's resilience against standardized wind and snow loads.

The application of finite element analysis as an active, in-service predictive maintenance tool is a relatively novel concept. Photovoltaic modules are composite structures comprising materials with vastly different coefficients of thermal expansion. A typical module consists of a tempered glass front layer, an upper layer of ethylene-vinyl acetate encapsulant, a matrix of interconnected silicon solar cells, a lower encapsulant layer, and a polymeric backsheet [14]. When an operational defect causes a localized thermal hotspot, the affected silicon cell attempts to expand rapidly. However, this expansion is constrained by the surrounding encapsulant and the rigid glass cover. This constraint generates significant thermal-mechanical stress. If the localized stress exceeds the yield strength or fracture toughness of the silicon or the encapsulant, it can initiate microcracking, propagate existing flaws, or cause delamination between the layers [15].

Previous studies that have modeled thermal stresses in solar panels typically rely on assumed, uniform temperature distributions or simplified, theoretical hotspot scenarios. The critical innovation explored in this research is the utilization of empirical, high-resolution thermal data captured by drone inspections as the direct input boundary conditions for the finite element simulation [16]. This direct linkage bridges the gap between field observation and computational mechanics. By mapping the real-world thermal footprint of a defect onto the computational model, the resulting stress analysis provides a highly accurate, physics-based evaluation of the module's immediate structural health and its propensity for future failure. This theoretical framework posits that integrating advanced computational mechanics into routine drone inspection workflows will dramatically refine maintenance prioritization, shifting the focus from simple thermal anomaly management to rigorous structural integrity preservation.

3. Methodology and Finite Element Modeling

3.1 Study Area and Drone Inspection Parameters

The empirical data for this study was collected from a utility-scale solar photovoltaic facility operating in a temperate climate zone, characterized by significant diurnal temperature variations. The selected inspection sector comprised approximately ten megawatts of installed capacity, featuring standard sixty-cell polycrystalline silicon modules mounted on fixed-tilt racking systems. The aerial data acquisition was executed utilizing a commercial-grade quadcopter equipped with a dual-sensor payload, specifically a high-definition visual camera and an uncooled microbolometer thermal infrared sensor. To ensure optimal thermal contrast, the flights were scheduled during the peak solar irradiance window, specifically between astronomical noon and early afternoon, under clear sky conditions with continuous solar irradiance exceeding a predefined threshold [17]. Wind speeds were monitored continuously and maintained below the operational limits to prevent excessive convective cooling of the module surfaces, which could skew the thermographic readings.

The flight path was autonomously managed via ground control station software, employing a standard lawnmower trajectory parallel to the axis of the solar arrays. The drone was configured to maintain a consistent altitude above the panel surface, calculated to yield a thermal ground sample distance suitable for resolving cell-level thermal anomalies. Both forward and lateral image overlap were set to high percentages to facilitate robust photogrammetric stitching and accurate temperature pixel matching. The camera gimbal was positioned at a near-nadir angle, optimized to capture the maximum thermal emission from the panels while avoiding specular reflections from the sun. Throughout the flight, the radiometric sensor recorded absolute temperature values embedded within the image metadata, which were calibrated against ambient temperature and humidity readings captured by a ground-based meteorological station.

Table 1: Mission Parameters for Aerial Thermographic Inspection

Parameter Category	Specific Configuration	Operational Purpose
Aerial Platform Settings	Fixed altitude, constant velocity	Ensure consistent spatial resolution and thermal measurement accuracy
Sensor Payload Configuration	Dual-band imaging, radiometric calibration	Capture synchronized visual and thermal data for comprehensive analysis
Flight Trajectory Planning	High overlap percentage, parallel paths	Facilitate seamless orthomosaic generation and precise defect localization
Environmental Constraints	High solar irradiance, low wind velocity	Maximize thermal contrast and minimize convective cooling effects

3.2 Data Acquisition and Processing Workflow

Following the completion of the aerial surveys, the raw radiometric imagery and associated visual data were offloaded into a high-performance computational environment for processing. The initial phase involved the application of photogrammetry algorithms to construct a spatially accurate, two-dimensional thermal orthomosaic of the entire inspected sector. This process utilized the precise spatial coordinates and inertial measurement unit data embedded in each image to align and stitch the thousands of individual photographs into a single, continuous map. Concurrently, a visual orthomosaic was generated to serve as a reference baseline [18].

The subsequent phase of the workflow focused on automated anomaly detection and extraction. Advanced image processing techniques were deployed to segment the thermal orthomosaic into individual panel boundaries. Within each segmented module area, a statistical analysis of the temperature distribution was conducted to identify pixels that deviated significantly from the mean operational temperature of the healthy surrounding cells. These localized temperature spikes were classified as hotspots. To isolate the most critical defects for further analysis, the system filtered the identified hotspots based on a predefined absolute temperature threshold and a relative temperature gradient criteria. For each selected hotspot, a high-resolution thermal profile was extracted, effectively creating a two-dimensional heat map matrix that represented the precise spatial distribution and intensity of the thermal anomaly across the surface of the specific solar panel. This empirical thermal matrix constituted the critical input dataset required for the subsequent structural simulation.

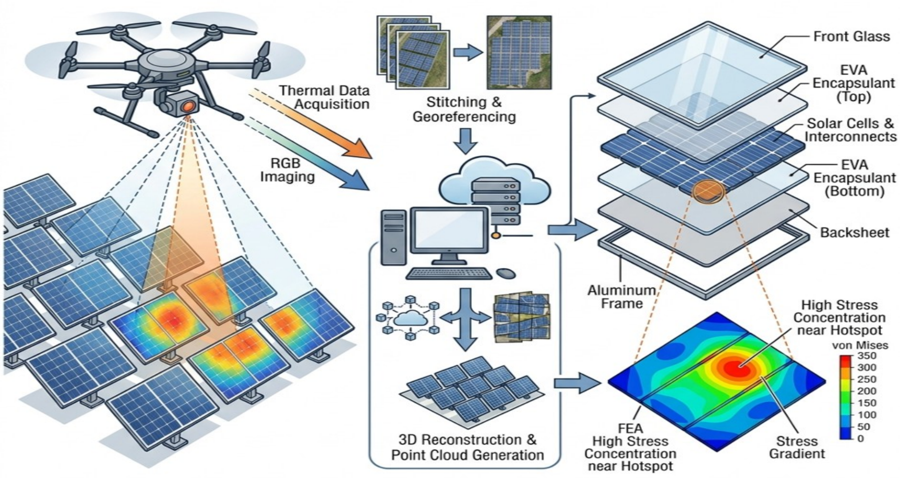

Figure 1: Comprehensive Schematic of Integrated Drone Inspection and Computational Stress Analysis Workflow

3.3 Finite Element Model Construction

The core of this methodology relies on the construction of a high-fidelity, three-dimensional finite element model representing the precise geometry and material architecture of the inspected photovoltaic modules. The geometric model was constructed using advanced computer-aided engineering software. The simulated panel was modeled as a composite sandwich structure consisting of five distinct layers. The uppermost layer was modeled as tempered low-iron glass, providing environmental protection and structural rigidity. Beneath the glass, the upper encapsulant layer was defined, followed by the active photovoltaic layer comprising interconnected polycrystalline silicon solar cells, inter-cell copper ribbons, and busbars. This was followed by the lower encapsulant layer and finally, the rigid polymeric backsheet.

To accurately simulate the physical response of this composite structure, precise material properties were assigned to each layer within the finite element solver. These properties included the modulus of elasticity, Poisson's ratio, thermal conductivity, specific heat capacity, and, crucially, the coefficient of thermal expansion [19]. The distinct differences in the coefficient of thermal expansion between the brittle silicon cells, the compliant polymeric encapsulant, and the rigid glass cover are the primary drivers of internal mechanical stress during temperature fluctuations. The computational mesh was generated using hexahedral solid elements, with a refined, high-density mesh applied specifically to the silicon layer and the interfaces between differing materials, as these regions are most susceptible to steep stress gradients and failure initiation.

The integration of the drone inspection data into the finite element model was achieved through a rigorous boundary condition mapping process. The two-dimensional thermal profile extracted from the drone imagery was mathematically interpolated and projected onto the surface nodes of the geometric model. This thermal load was applied in conjunction with standard convective and radiative heat transfer boundary conditions applied to the front and rear surfaces of the panel model to simulate interaction with the ambient environment.

The mechanical boundary conditions constrained the edges of the model to simulate the rigid clamping of the panel to the aluminum mounting structure. The finite element solver then executed a coupled thermal-structural analysis. Initially, it calculated the three-dimensional steady-state temperature distribution throughout the depth of the module layers. Subsequently, it computed the resulting mechanical deformation, strain, and complex triaxial stress fields, specifically focusing on the generation of von Mises equivalent stresses within the fragile silicon matrix and the shear stresses at the material interfaces, which are indicative of impending delamination or microcrack propagation [20].

4. Results and Analytical Discussion

4.1 Thermographic Defect Identification Outcomes

The initial phase of data analysis focused on the spatial distribution and thermal characteristics of the anomalies identified during the drone inspection. The aerial thermography successfully surveyed thousands of modules, detecting a wide spectrum of thermal irregularities. The most frequently observed anomalies included localized cellular hotspots, string-level heating indicative of bypass diode activation or failure, and broader thermal gradients associated with severe surface soiling or structural shading. By cross-referencing the radiometric data with the high-resolution visual imagery, false positives were effectively eliminated.

The empirical thermal data revealed that localized cellular defects often exhibited extreme temperature differentials. In several instances, individual cells recorded temperatures significantly higher than the average operating temperature of adjacent healthy cells. These acute hotspots are typically symptomatic of severe internal resistance caused by phenomena such as reverse bias heating, where a shaded or damaged cell acts as a resistor rather than a generator, dissipating current from the rest of the string as intense localized heat. The extracted thermal matrices provided a highly precise contour map of these heat concentrations, demonstrating that the temperature distribution was rarely uniform across a defective cell. Instead, the heat was often concentrated near the busbars or along the paths of preexisting, visually undetectable microcracks. This granular thermal mapping underscored the limitation of using a single maximum temperature value to characterize a defect and reinforced the necessity of importing the complete spatial thermal profile into the subsequent structural simulation.

4.2 Thermal-Mechanical Stress Analysis via Finite Element Modeling

The application of the drone-derived thermal data to the finite element model yielded profound insights into the hidden structural consequences of operational hotspots. The computational results demonstrated that significant temperature gradients on the module surface translated into severe, multi-axial mechanical stress within the internal layers. The most critical findings emerged from the analysis of the von Mises stress distribution within the polycrystalline silicon layer. Because the silicon cells are tightly encapsulated between the glass and the backsheet, their natural thermal expansion is heavily restricted. When subjected to the localized thermal loads extracted from the drone data, the simulation revealed intense stress concentrations forming at the boundaries between the overheated cell and the cooler surrounding materials.

The finite element analysis indicated that the magnitude of the induced mechanical stress was directly proportional to the spatial steepness of the temperature gradient rather than the absolute peak temperature alone. For example, a concentrated hotspot with a rapid temperature drop-off toward the cell edges generated significantly higher localized shear and tensile stresses than a broader, more diffuse thermal anomaly of the same peak temperature. In several modeled scenarios based on severe field-detected hotspots, the calculated internal stresses approached or exceeded the established fracture strength of typical polycrystalline silicon. This computational evidence strongly suggests that these specific thermal anomalies are not merely electrical inefficiencies but are actively propagating microstructural damage. Furthermore, the analysis of the interfacial shear stresses between the silicon cells and the encapsulant layers indicated a high probability of localized delamination in the vicinity of severe hotspots. Such delamination would further exacerbate the issue by degrading thermal dissipation, leading to a destructive positive feedback loop of increasing temperature and accelerating mechanical failure.

Table 2: Impact of Integrated Workflow on Maintenance Metrics

Operational Metric	Traditional Inspection Paradigm	Integrated Drone and Finite Element Workflow
Defect Categorization Basis	Surface temperature differential alone	Computationally derived structural stress
Maintenance Intervention Strategy	Reactive replacement based on broad criteria	Targeted intervention based on failure probability
Resource Deployment Efficiency	Extensive manual verification required	Highly optimized, data-driven labor allocation
Lifecycle Management Focus	Short-term electrical output restoration	Long-term structural integrity and yield preservation

4.3 Impact on Maintenance Efficiency and Resource Allocation

The translation of finite element modeling results into actionable maintenance intelligence represents a fundamental paradigm shift for solar farm operations. Under conventional drone inspection workflows, a maintenance manager presented with a report detailing hundreds of hotspots of varying temperatures faces a complex triage challenge. Often, modules are flagged for replacement based on arbitrary temperature thresholds, a strategy that inevitably results in the premature disposal of panels that may possess stable, non-critical thermal variations while inadvertently ignoring lower-temperature anomalies that happen to induce critical stress concentrations near mounting points.

By integrating finite element analysis into the diagnostic pipeline, operators acquire a predictive dimension that explicitly links thermal data to physical degradation. The structural simulation acts as a highly advanced analytical filter, stratifying detected anomalies based on their calculated potential to cause immediate or near-term mechanical failure. This allows maintenance teams to prioritize interventions with unprecedented precision. A hotspot that the finite element model indicates is generating stress levels near the silicon fracture point can be immediately escalated for priority replacement to prevent sudden string failure or fire hazards. Conversely, thermal anomalies that generate negligible structural stress, even if exhibiting elevated temperatures, can be relegated to routine monitoring schedules.

This physics-based prioritization drastically improves maintenance efficiency. It optimizes resource allocation by directing technical personnel only to locations requiring critical intervention, thereby reducing unnecessary labor costs and minimizing the operational downtime associated with unwarranted panel replacements. Furthermore, this integrated approach enhances inventory management, as procurement can be aligned with the predictive failure rates generated by the structural simulations rather than relying on historical averages or reactive purchasing. Ultimately, linking drone inspection workflows to finite element modeling transforms solar farm maintenance from a descriptive exercise into a prescriptive, structurally informed strategy that safeguards the asset's overall lifecycle and maximizes sustainable energy production.

5. Conclusion and Implications

5.1 Summary of Findings

This comprehensive study has successfully demonstrated the profound theoretical and practical benefits of linking autonomous drone inspection workflows with advanced finite element modeling in the context of utility-scale solar farm operations. The research establishes that while aerial thermography is an exceptionally rapid and scalable method for acquiring diagnostic data across vast photovoltaic arrays, the reliance on surface temperature differentials alone provides an incomplete and potentially misleading assessment of module health. By extracting high-resolution thermal matrices from empirical drone data and applying them as boundary conditions within a multi-layered computational simulation, this study illuminated the hidden mechanical dynamics occurring within the solar panels. The finite element analysis clearly revealed that concentrated thermal anomalies generate severe, highly localized thermal-mechanical stress fields within the fragile silicon cells and at the encapsulant interfaces. Crucially, the research found that the spatial gradient of the thermal anomaly, rather than just its peak temperature, is the primary driver of critical structural stress capable of initiating microcracking or delamination. This computational evidence bridges the vital gap between remote diagnostic observation and predictive structural health assessment.

5.2 Strategic Maintenance Implications

The integration of computational solid mechanics into routine renewable energy maintenance workflows holds significant strategic implications for the solar industry. This synergistic methodology empowers solar farm operators to transition decisively from reactive or threshold-based maintenance paradigms to sophisticated, condition-based predictive strategies. By utilizing finite element modeling as an analytical filter, asset managers can accurately quantify the structural severity of every detected hotspot, enabling highly precise prioritization of maintenance interventions. This capability directly enhances overall operational efficiency by minimizing unnecessary field deployments, optimizing the allocation of technical labor, and reducing unwarranted equipment replacement costs. Furthermore, by addressing structurally critical defects before they precipitate catastrophic module failure or cascading string outages, this integrated approach preserves the overall health of the photovoltaic infrastructure. As global reliance on solar energy continues to escalate, the deployment of intelligent, physics-informed maintenance frameworks will be paramount. Future advancements in automated data pipelines and cloud-based computational mechanics will likely enable real-time stress analysis during drone flight operations, further solidifying the indispensable role of integrated diagnostic methodologies in maximizing the longevity, safety, and economic viability of utility-scale solar power generation [21].

References

1. Cheng, D.; Gao, Y.; Yang, C. A Comprehensive Review on Wafering of Silicon Substrate for Photovoltaic Solar Cell. Sol. Energy 2025, 301, 113977.

2. Ramaswamy, M.; Palaniswamy, S. Multimodal Emotion Recognition: A Comprehensive Review, Trends, and Challenges. Wires Data Min. Knowl. Discov. 2024, 14, e1563.

3. Yao, Y.; Cao, X.; Liu, X.; Zhang, Z.; Xu, W.; Wen, H. A comprehensive review of solid-state friction stir processing robots: Design, dynamics and control for enabling applications in additive manufacturing. J. Manuf. Process. 2025, 149, 1151–1165.

4. Guerrero, L.A.; Vásquez, F.; Ochoa, S.F. An Indoor Navigation System for the Visually Impaired. Sensors 2012, 12, 8236–8258.

5. Mohr, D.C.; Schueller, S.M.; Montague, E.; Burns, M.N.; Rashidi, P. The Behavioral Intervention Technology Model: An Integrated Conceptual and Technological Framework for eHealth and mHealth Interventions. J. Med. Internet Res. 2014, 16, e146.

6. Miranda, G.; Faria, S.; Bartolomeu, F.; Pinto, E.; Alves, N.; Silva, F.S. The Influence of Laser Power and Scan Speed on the Dimensional Accuracy of Ti6Al4V Thin-Walled Parts Manufactured by Selective Laser Melting. Metals 2022, 12, 1226.

7. Liu, F.; Li, J.; Cao, S.; Liu, B.; Zhang, Y. Mechanism of Grinding Depth Induced Carbonization Damage in GPLIM Processing of SiC Wafers with Backside Metal Layers. J. Alloys Compd. 2025, 1048, 185249.

8. Zheng, Z.; Lin, X.; Zhao, Z.; Lin, Q.; Liu, J.; Chen, M.; Wu, W.; Wu, Z.; Liu, N.; Chen, H. A vascular endothelial growth factor–loaded chitosan-hyaluronic acid hydrogel scaffold enhances the therapeutic effect of adipose-derived stem cells in the context of stroke. Neural Regen. Res. 2025, 20, 3591–3605.

9. Wang, H.; Chen, Z.; Kozinets, G.; Kozinets, P.; Markov, A.; Cao, P. Multi-strategy improved snake optimization algorithm for predicting the ice melting rate of a thermal coring bit. Int. J. Heat Mass. Transf. 2025, 252, 127491.

10. Chung, C.-Y. Integrated Optimum Layout of Conformal Cooling Channels and Optimal Injection Molding Process Parameters for Optical Lenses. Appl. Sci. 2019, 9, 4341.

11. Krizhevsky, A.; Sutskever, I.; Hinton, G.E. ImageNet Classification with Deep Convolutional Neural Networks. In Proceedings of the Advances in Neural Information Processing Systems, Lake Tahoe, NV, USA, 3–6 December 2012; pp. 1097–1105.

12. Vaswani, A.; Shazeer, N.; Parmar, N.; Uszkoreit, J.; Jones, L.; Gomez, A.N.; Kaiser, Ł.; Polosukhin, I. Attention Is All You Need. In Proceedings of the Advances in Neural Information Processing Systems, Long Beach, CA, USA, 4–9 December 2012; pp. 5998–6008.

13. Zhou, X.; Tao, C.; Liang, X.; Liu, Z.; Li, H. Design and Mechanical Properties of Maximum Bulk Modulus Microstructures Based on a Smooth Topology with Grid Point Density. Aerospace 2024, 11, 145.

14. Alarifi, I.M. A performance evaluation study of 3d printed nylon/glass fiber and nylon/carbon fiber composite materials. J. Mater. Res. Technol. 2022, 21, 884–892.

15. Rudnik, M.; Szot, W.; Kowalska, N.; Szczygiel, P. Bending Properties of Standardized Photopolymer-Silicone Hybrid Structures Manufactured via PolyJet Matrix. Materials 2025, 18, 5612.

16. Chen, Z.; Li, F.; Liu, W.; Zhang, Y.; Zhang, Q. Temperature Distribution Simulation and Laser Performance of Nd:YAG Composite Laser Crystals. Results Opt. 2025, 21, 100899.

17. Carton, L.; Riva, R.; Nélias, D.; Fourmeau, M. Weibull Strength Size Effect of Diamond Wire Sawn Photovoltaic Silicon Wafers. J. Eur. Ceram. Soc. 2020, 40, 5357–5368.

18. Abbas, F.; Belkhir, N.; Herrmann, A.; Rädlein, E. Investigation of the Impact of Optical Glass Composition on Ceria Slurry Stability during Chemical Mechanical Polishing Process. Powder Technol. 2024, 448, 120290.

19. Dong, H.; Gao, Y.; Yang, C. Surface and Subsurface Microstructure Properties of Monocrystalline Silicon Cut by Electroplated Diamond Wire Saw. Surf. Sci. Technol. 2025, 3, 30.

20. Huang, J.; Kang, R.; Dong, Z.; Gao, S. Prediction Model for Surface Shape of YAG Wafers in Wafer Rotational Grinding. Int. J. Mech. Sci. 2025, 287, 109982.

21. Zhu, Y.; Liu, F.; Wang, Y.; Zhang, H.; Xue, P.; Wu, L.; Ni, D.; Xiao, B.; Ma, Z. Fabrication of Thin-Walled Metal Structures with Enhanced Energy Absorption Capabilities by Metal-Fused Deposition Modeling without Using Debinding Chemical Reagents. Adv. Eng. Mater. 2025, 27, 2402792.